

Robust Channel Assignment for Link-level Resource Provision in Multi-Radio Multi-Channel Wireless Networks

Cunqing Hua, Song Wei and Rong Zheng

Department of Computer Science, University of Houston, Houston, TX 77204

Email: {cqhua, swei, rzheng}@cs.uh.edu

Abstract—In this paper, we investigate the problem of link-level resource provision in multi-radio multi-channel (MR-MC) wireless networks. To quantify robustness of resource provision schemes, we propose the novel concept of *interference margin*. Using the notion of interference margin, a robust radio and channel assignment problem is formulated that explicitly takes into consideration link-level traffic demands. The key advantage of the proposed formulation is its robustness to channel variability and co-existence of external interference sources. We utilize the generalized Benders decomposition techniques to decouple the radio and channel assignment (combinatorial constraints) and network resource allocation (continuous constraints) so that the problem can be solved efficiently. The proposed algorithm is guaranteed to converge to the optimal solution within a finite number of iterations. We have evaluated our scheme using traces collected from a wireless mesh testbed and simulation studies in Qualnet. Experiments show that the proposed algorithm is superior to existing schemes in providing larger interference margin, and reducing outage and packet loss probabilities.

I. INTRODUCTION

In the past decade, WiFi technologies have been very successful in delivering best-effort broadband access in homes, campus and small businesses. However, current WiFi infrastructure is inadequate in supporting QoS-sensitive applications seamlessly across mobile and fixed access networks (e.g., Ethernet), such as VoIP, video streaming and on-line gaming. Similar requirements also arise from medical and industrial control domains for cable replacement solutions that can achieve reliable and timely delivery of control and application data comparable to existing wired counter-parts. Interestingly, the challenging aspects of afore-mentioned applications do not come from the scale of the networks, as in most cases, the wireless devices only have limited hop distance (one or two) to a backbone wireline network. Rather, the difficulty is the lack of effective means to manage interference caused by co-existing communication end-points and networks, as well as Electro-Magnetic Interference (EMI) sources in the environment.

In this paper, we investigate the problem of link-level resource provision in multi-radio multi-channel (MR-MC) wireless networks. In particular, we consider how to make channel assignment decisions to meet given link-level traffic demands. We argue that a *robust* link-level resource provision solution, which can provide a service abstraction similar to

that of a wired cable, will greatly simplify the design of upper layer routing and transport protocols. Instead of coping with the complexity caused by wireless channel dynamics using complicated cross-layer approaches, one can instead focus on network and system level issues of intended applications. To make our discussion more concrete, let us consider two application scenarios.

- A visual surveillance network consisting of many spatially distributed *smart cameras* inter-connected by wireless interfaces. Due to the limited field of view and resource constraints of individual nodes, collaborative in-network processing is required in order to continuously track the movement of interested objects. Features of objects need to be handed off between neighboring cameras to carry out vision tasks in a peer-to-peer manner. Based on the characteristics of the capture devices and vision algorithms, one can often determine ahead of time the bandwidth requirements among the cameras.
- A smart environment application (e.g., in assisted living facilities) that tracks vital signs of its habitants. Biosensors such as multi-channel EEG, EKG sensors typically samples at a fixed data rate and reports the measurements to medical personnel via wireless access points.

Both applications can be abstracted as a network of nodes inter-connected by a set of links, each associated with a *quasi-static* bandwidth requirement (with the difference that the former forms a mesh topology whereas the later is best modeled as a star topology). In the paper, we consider a general setting where each wireless node is equipped with multiple radios, which are capable of switching between different channels. As a result, each link can choose to associate with any radio interface at its transmitter and receiver nodes, and operate in any available channel. A radio and channel assignment solution is needed to determine the radio and channel association. This assignment decision should be made at *coarse time granularity* on a *per-link* basis rather than on a per-packet basis to mitigate channel switching cost. It should be made robust to the dynamics of wireless channels and interference from external network sources as the later is unmanageable in general. When restricted to single radio devices, the solution should still be applicable.

In this paper, we propose a radio and channel assignment algorithm that takes into consideration realistic channel conditions, network resource constraints and link-level demand.

This work is funded in part by the National Science Foundation (NSF) under award CNS-0832084 and the Grants to Enhance and Advance Research Program (GEAR) at the University of Houston.

We define a novel concept called “interference margin” that quantifies the robustness of channel assignment schemes. Interference margin reflects the allowance toward fluctuating link condition and unmanageable interferences while sustaining the desired level of quality of service. The major challenge in robust link-level resource provision is to incorporate the radio and channel allocation (combinatorial constraints), and network resource (continuous constraints) in a single optimization framework, which is known to be NP-hard in general [16]. Existing solutions using relaxed linear programming [20], the minimum coloring algorithm [22] and heuristic algorithms [2], [9] either do not account for traffic demands or can only offer approximate results. We address this problem by proper transformation and imposing a special structure. The generalized Benders decomposition technique [5] is then applied to decompose the optimization problem to a primal problem and a master problem. The primal problem is obtained by fixing the binary variables from the original problem, and the master problem is obtained via nonlinear duality theory for the solution of binary variables. The proposed algorithm is guaranteed to converge to the optimal solution within a finite number of iterations.

Using traces collected from a wireless mesh testbed, we conduct a set of experiments to evaluate the performance of the proposed radio and channel assignment algorithm and compare it with other existing schemes. We also incorporate the trace data in the Qualnet simulator and compare the performance of several algorithms through simulation study. The experiments show that the proposed algorithm is superior to existing schemes in providing larger interference margin, and reducing outage and packet loss probability. We also demonstrate the convergence behavior of our algorithm.

Main contribution: In this paper, we make the following contributions.

- A novel concept of *interference margin* is proposed as a quantitative measure for robustness of link-level resource provision.
- A new channel assignment scheme for MR-MC networks is designed with several advantageous features: i) explicitly accounting for link-level demand, ii) incorporating measurement-driven interference and link capacity model; iii) robustness to external interference and fluctuation of channel gains, and iv) provable convergence to global optimality.

The rest of this paper is organized as follows. In Section II, we provide a categorization of existing work. The models assumed and the problem statement are formally defined in Section III. A radio and channel allocation algorithm is presented in Section IV. Evaluation using real-world trace data from our mesh testbed and simulation is presented in Section V and Section V-C. Finally, we conclude the paper with future research avenue in Section VI.

In this section, we review existing channel allocation schemes that are most pertinent to this paper, which are classified based on several criteria detailed next.

- **Traffic-agnostic vs traffic-aware channel assignment**

Traffic-agnostic channel assignment approaches assume uniform distribution of traffic among all links and try to minimize the overall interference. In [8], Bruno *et al.* propose the channel selection and user association algorithms to minimize the inter-AP interference of 802.11 WLANs. The algorithms utilize the *Gibbs sampler* technique, which can be implemented distributively with locally measurable quantities such as interference and transmission delay. However, the proposed algorithms do not consider the traffic demand between APs and clients. In [20], Subramanian *et al.* consider the channel assignment problem for minimizing interference in MC-MR mesh networks. They propose a centralized heuristic algorithm based on Tabu search approach and a distributed algorithm using greedy approximation for uniform traffic demands. The generalization to heterogeneous link-level demands and overlapping channels using a weighted form is suggested in the paper. However, no explicit guarantee can be provided.

Along the line of traffic-aware channel assignment, Raniwala *et al.* [16] present a centralized load-aware channel assignment and multipath routing algorithm. They propose to give a higher priority to heavy-loaded links in channel assignment. However, this algorithm is based on heuristics and its optimality is unclear. In [18], several traffic-aware metrics are proposed that incorporate demands with the channel separation metrics for wireless LANs. Larger weights are assigned to APs with higher loads. The channel allocation algorithms try to maximize the weighted channel separation by allocating channels with larger separation to APs with higher loads.

- **Binary vs physical interference and link capacity model**

Most channel assignment algorithms require interference information as inputs. Recent studies [12], [17] show that some well-accepted propagation models are inaccurate for prediction of link-level interference, especially in the indoor environment where the radio signal degrades much faster than that in free space environment. Therefore, there has been some recent work that incorporate the measurement results into the interference modeling and link capacity prediction [7], [13]. Based on the measurements, the work in [9], [16], [18], [20] builds a binary conflict graph, wherein each link is represented by a vertex, and an edge exists between two vertices if the two links interfere with one another. A binary interference model is inaccurate as shown from the measurement results in [12], [17]. The sustainable transmission rate to successfully decode packets can be impacted by stations outside carrier sensing range.

In [8], a channel algorithm is designed based on the mea-

	Centralized	Distributed
Traffic-aware	[2], [9], [16], [18]	
Traffic-agnostic		[8], [20]
Binary conflict graph	[2], [9], [14], [16], [18]	[20]
Physical interference and link capacity		[8]

TABLE I: Classification of channel assignment algorithms

surement quantities such as interference and transmission delay. However, this work assumes a symmetric channel so that the bi-directional interference can be measured locally, which may not hold in practice. In this paper, we adopt a hybrid model that closely characterizes the behavior of the IEEE 802.11 protocol. Two nodes are in direct conflict and thus cannot transmit concurrently (e.g., due to carrier sensing) if the received signal at the other nodes is higher than a certain threshold. On the other hand, distant transmitters operating in the same channel contribute to the signal-noise-and-interference-ratio, which leads to lower transmission rate.

- **Centralized and distributed schemes** In [9], Kodialam *et al.* present channel assignment and routing algorithms to characterize the capacity regions of a MR-MC mesh networks. The problem of throughput maximization for a MR-MC network is considered in [2]. Unlike our proposed scheme, the work in [2], [9] focuses on optimizing end-to-end throughput, which require to jointly optimize channel assignment, routing and scheduling. Therefore, the algorithms cannot be easily implemented in a distributed manner. In [14], Rad *et al.* formulate the joint channel allocation, interface assignment and media access control problem as a non-linear mixed-integer network utility maximization problem. They assume that a wireless interface is dedicated to a single channel if it is assigned to multiple links, while our work allows the interface to switch between different channels to serve different links. Our work also differs from this work in that we solve the mixed-integer programming problem using the generalized Benders decomposition technique, which is guaranteed to converge to the optimal solution.

A summary of the related work and their respective categorization can be found in Table I.

III. MODELS AND PROBLEM STATEMENT

A. Overview

The network considered in this paper is a MR-MC wireless network consisting of a set of directed links \mathcal{L} . A link $l = (s, t)$ is in \mathcal{L} if and only if: (i) packets from transmitter node s to receiver node t are *decodable* in absence of interference from other links; (ii) there is a non-negative link-level demand A_l associated with link l . For example, in visual surveillance application, the link demand is the maximum data rate for inter-camera communications over the link.

Each node s has R_s radios, each of which can switch between K orthogonal channels. We assume $R_s \leq K$ since it is not useful to operate multiple radios on the same channel simultaneously. For a node where the number of incident links

is larger than the number of its radios, some of its radios will be shared by multiple links.

We assume that each link is associated with a unique pair of radios at the transmitter and receiver nodes and a single channel. This formulation can be extended to the case when multiple radios are used concurrently to support the demand between a pair of transmitter and receiver nodes by introducing multiple logical links. For each link l , three *binary* variables are defined to characterize the assignment of radios and channel:

- x_l^i : equals 1 if radio i is assigned to link l at transmitter node s , and 0 otherwise.
- y_l^j : equals 1 if radio j is assigned to link l at receiver node t , and 0 otherwise.
- z_l^k : equals 1 if channel k is assigned to link l , and 0 otherwise.

Since each link can only use one transmitting radio and receiving radio, and one channel at each time, the following constraints should hold for any feasible radio and channel assignment solution,

$$\sum_{i \in R_s} x_l^i = 1, \sum_{j \in R_t} y_l^j = 1, \text{ and } \sum_{k \in K} z_l^k = 1, \forall l \in \mathcal{L} \quad (1)$$

Let $s(l)$, $t(l)$ be the transmitter and receiver node of link l . x , y , z are multisets of elements $\{x_l^i\}$, $\{y_l^j\}$, $\{z_l^k\}$, for $i = \{1, 2, \dots, R_{s(l)}\}$, $j = \{1, 2, \dots, R_{t(l)}\}$, $k = \{1, 2, \dots, K\}$.

B. Radio and contention constraints

We assume all radios are *half-duplex*, so if two links are associated with the same radio interface, they should be scheduled to different time slots since only one link can be served by the radio at each time. In addition, any two links within the same spatial contention domain and sharing the same channel cannot transmit simultaneously if the transmission of one of them lead to excessive interference and thus the reception failure of the other link.

Characterization of contention relationship in wireless networks is a long standing problem. The main challenge comes from trade-offs among complexity, schedulability and capacity region. For instance, clique constraints (which are simpler to derive) are often used in optimization formulations [6], but the resulting flow vectors are not always schedulable; solutions using independent set constraints yield schedulable flow vectors but generally incur non-polynomial compute complexity [6]. Maximal scheduling [4], [21] based on local information, on the other hand, is always feasible but has been shown to have reduced capacity region in general (with the exception when the ‘‘local pooling’’ condition [23] is met).

In this paper, we adopt the set of constraints in line with maximal scheduling, which yields simple distributed scheduling similar to the IEEE 802.11 DCF though we believe the formulation can be readily extended to other forms of contention characterization. Let I_l^s and I_l^t denote the set of links sharing the same node with link l at the transmitting node s and the receiving node t , and I_l^c as the set of links in the same contention domain with link l in a *single radio and single channel* network (Fig. 1). Let C_l denote the effective

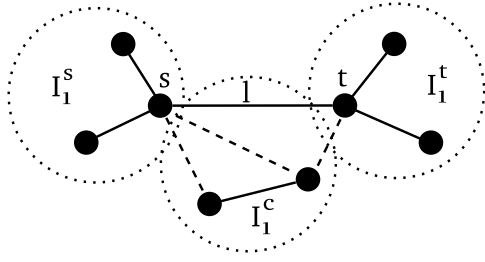


Fig. 1: Radio and channel contention links

link rate of link l , then the time to satisfy the traffic demand of link l is given by A_l/C_l . Consider contention from all links sharing the same radios or channel, the aggregate transmission time of link l (operating in radio i , j and channel k) and all its contending links is bounded by

$$T_l(x, y, z) = \frac{A_l}{C_l} + \sum_{v \in I_l^s} \frac{x_v^i A_{lv}}{C_{lv}} + \sum_{v \in I_l^t} \frac{y_v^j A_{lv}}{C_{lv}} + \sum_{v \in I_l^c} \frac{z_v^k A_{lv}}{C_{lv}} \quad (2)$$

In the worst case, any two of these links are conflicting with each other, so they should be scheduled at different time. Therefore, it is required that

$$T_l(x, y, z) \leq 1, \forall l. \quad (3)$$

The right hand side of the above inequality can be replaced by a factor κ ($\kappa \geq 1$) to reflect the looseness of maximal scheduling constraints resulting in a tighter capacity region. However, schedulability is not always guaranteed when $\kappa > 1$.

C. Interference margin and effective link rate

We consider the generalized physical interference model and assume that when a node is transmitting to its intended receiver, all other concurrent transmissions are treated as interference. In this model, the effective link rate C_l of link l is a function of the signal-to-interference-plus-noise ratio (SINR) at the receiver, or $C_l = f(\text{SINR}_l)$. Let P_s denote the transmission power of node s , G_{st} denote the channel gain of link (s, t) , σ_0 denote the noise floor, and σ_e denote the external interference, then the SINR is given by

$$\text{SINR}_l = \frac{P_s G_{st}}{\sigma_0 + \sigma_e + \sum_{s' \neq s} P_{s'} G_{s't}}$$

There are two sources of variability for this model. First, the channel gain between the transmitter and receiver is subject to large-scale and small-scale fading due to signal attenuation over distance, shadowing, and multipath effects etc.. The second are external interferences from devices operating in overlapping spectrum. Examples are co-existing WLANs, WPANs and other EMI sources. The variations of channel gain and external interferences are generally unmanageable, and the interference level is difficult to predict.

To capture the effects of channel dynamics and external interference, we introduce the novel concept of *interference margin* as a quantitative measure to characterize robustness to channel and external interference variability. Specifically, we define an *interference margin* σ_l for each link l , which represents the *maximum channel and external interference*

variability that can be tolerated to sustain the targeted transmission rate for the link. It can also be understood as the equivalent interference as a result of the dynamic of channel and external interference. Thus, we can rewrite the SINR as a function of the *mean* channel gain \bar{G}_{st} and the *interference margin* as

$$\text{SINR}_l = \frac{P_s \bar{G}_{st}}{\sigma_0 + \sigma_l + \sum_{s' \neq s} P_{s'} \bar{G}_{s't}}$$

\bar{G}_{st} will be obtained through measurement data.

D. Robust radio and channel assignment problem

Our objective is to allocate the radios and channels for all links such that the link demands remain satisfied in presence of moderate channel dynamics. Intuitively, the larger the interference margin, the more robust the resulting radio and channel assignment to channel variability and external interferences. The problem is thus to find the set of radio and channel assignment for all links so as to maximize the interference margin of all links subject to certain fairness properties.

To this end, we define a utility function U_l for each link l , which is a function of the *interference margin* σ_l and has the following properties: (i) the utility function $U_l(\sigma_l)$ is increasing, strictly concave and 2nd order differentiable; (ii) $U_l(\sigma_l)$ is additive so that the aggregated utility of all links is $\sum_{l \in \mathcal{L}} U_l(\sigma_l)$. Different utility functions have been defined for different fairness models, such as proportional fairness and max-min fairness [15].

The problem can be formally stated as a network utility maximization problem, which is a mixed integer nonlinear programming problem (MINLP) as follows,

$$\begin{aligned} \max \quad & \sum_{l \in \mathcal{L}} U_l(\sigma_l) \\ \text{s.t.} \quad & T_l(x, y, z, \sigma) \leq 1, \forall l \in \mathcal{L}, \\ & x_l^i, z_l^j, x_l^k = \{0, 1\}, \forall l \in \mathcal{L}, \\ & \sigma_l \geq 0, \forall l \in \mathcal{L}. \end{aligned} \quad (4)$$

In Eq. (4), $T_l(x, y, z, \sigma)$ is determined by channel assignment variables and the effective link rate C_l (Eq.(2)), which in turn is a function of the interference margin. In the following, a general form of link capacity is assumed in the discussion of the solution approach, the special form of link capacity in additive white Gaussian noise (AWGN) channel will be used to derive numerical solutions. Solutions to MINLP problems in (4) give the radio and channel assignment results x, y, z , as well as the interference margin σ . By using the lowest feasible rate (subject to link level demands), the utility of interference margin is maximized; and thus the resulting radio and channel assignment is robust to channel variation and external interference.

IV. ROBUST RADIO AND CHANNEL ASSIGNMENT ALGORITHM

In general, a MINLP problems defined in (4) is known to belong to NP-hard problems and no efficient solutions

exist because the complexity may increase exponentially with problem size. However, in some practical applications, the MINLP problem often possesses certain special structures that can be exploited for designing effective solutions. One special situation is that the problem is not convex with respect to continuous and discrete variables jointly, but fixing the discrete variables renders them so for continuous variables. The generalized Benders decomposition (GBD) [5] has been proposed for MINLP problem with this property.

A. Generalized Benders decomposition

The basic idea of the GBD algorithm is to decompose the original MINLP problem to a *primal* problem and a *master* problem and solve them iteratively. The *primal* problem corresponds to the original problem with fixed binary variables, solving this problem provides the information about the *lower* bound and the Lagrange multipliers corresponding to the constraints. The *master* problem is derived through nonlinear duality theory using the Lagrange multipliers obtained from the primal problem. The solution to the master problem gives the information about the *upper* bound as well as the binary variables that can be used for primal problem in next iteration.

1) *Primal problem*: Consider the MINLP problem in (4), the primal problem is obtained as follows by fixing the binary variables to $(\hat{x}, \hat{y}, \hat{z})$:

$$P(\hat{x}, \hat{y}, \hat{z}) \begin{cases} v(\hat{x}, \hat{y}, \hat{z}) = \max & \sum_{l \in \mathcal{L}} U_l(\sigma_l) \\ \text{s.t.} & T_l(\hat{x}, \hat{y}, \hat{z}, \sigma) \leq 1, \forall l \in \mathcal{L}, \\ & \sigma_l \geq 0, \forall l \in \mathcal{L}. \end{cases}$$

where $v(\hat{x}, \hat{y}, \hat{z})$ is the value function of the primal problem $P(\hat{x}, \hat{y}, \hat{z})$. Since the optimal solution of this problem is also a feasible solution to problem (4), the optimal value $v(\hat{x}, \hat{y}, \hat{z})$ provides a lower bound to the original problem.

In general, not all choices of the binary variables lead to a feasible primal problem. It should be treated differently depending on whether the primal problem is feasible or not:

• Feasible Primal

If the primal problem is feasible, we can form the Lagrange function for the primal problem as

$$L(\hat{x}, \hat{y}, \hat{z}, \sigma, \lambda) = \sum_{l \in \mathcal{L}} U_l(\sigma_l) + \sum_{l \in \mathcal{L}} \lambda_l (1 - T_l(\hat{x}, \hat{y}, \hat{z}, \sigma)) \quad (5)$$

where $\lambda_l \geq 0$ is the multiplier for the constraint of link l . The dual problem is thus

$$\min_{\lambda \geq 0} \max_{\sigma \geq 0} L(\hat{x}, \hat{y}, \hat{z}, \sigma, \lambda) \quad (6)$$

• Infeasible Primal

If the primal problem is infeasible, we define a set V as

$$V = \{\hat{x}, \hat{y}, \hat{z} | T_l(\hat{x}, \hat{y}, \hat{z}, \sigma) \leq 1, \text{ for some } \sigma_l \geq 0\}$$

and consider the following feasibility-checking problem

$$F(\hat{x}, \hat{y}, \hat{z}) \begin{cases} v_0(\hat{x}, \hat{y}, \hat{z}) = \min_{\sigma \geq 0} \sum_{l \in \mathcal{L}} w_l T_l^+(\hat{x}, \hat{y}, \hat{z}, \sigma) \\ \text{s.t.} & T_l(\hat{x}, \hat{y}, \hat{z}, \sigma) \leq 1, \forall l \in \mathcal{L}. \end{cases}$$

where $T_l^+ = \max(0, T_l)$. The weights w_l s are nonnegative and not all zero, and $w_l = 0$ if $T_l(\hat{x}, \hat{y}, \hat{z}, \sigma)$ does not attain the maximum value. Then the Lagrangian function for the infeasible primal problem can be defined as

$$G(\hat{x}, \hat{y}, \hat{z}, \sigma, \mu) = \sum_{l \in \mathcal{L}} \mu_l (T_l(\hat{x}, \hat{y}, \hat{z}, \sigma) - 1) \quad (7)$$

It is shown in [5] that $(\hat{x}, \hat{y}, \hat{z})$ belong to the set V if and only if they satisfy the following system:

$$0 \geq \min_{\sigma \geq 0} G(\hat{x}, \hat{y}, \hat{z}, \sigma, \mu), \forall \mu \in \Lambda$$

$$\text{where } \Lambda = \{\mu_l \geq 0, \sum_{l \in \mathcal{L}} \mu_l = 1.\} \quad (8)$$

2) *Master problem*: The original problem in (4) can be written as

$$\begin{aligned} \max_{\sigma, x, y, z} \sum_{l \in \mathcal{L}} U_l(\sigma_l) &= \max_{x, y, z} v(x, y, z) \\ &= \max_{x, y, z} (\min_{\lambda \geq 0} \max_{\sigma \geq 0} L(x, y, z, \sigma, \lambda)) \\ &= \max \beta \\ \text{s.t.} & \beta \leq \max_{\sigma \geq 0} L(x, y, z, \sigma, \lambda), \forall \lambda_l \geq 0, \\ & x_l, y_l, z_l \in \{0, 1\} \cap V, \forall l \in \mathcal{L}. \end{aligned} \quad (9)$$

where the first equality is obtained from (6). Incorporating (8) into (9), we can make the constraints over set V explicit and obtain the following master problem:

$$\begin{aligned} \max \beta \\ \text{s.t.} & \beta \leq \max_{\sigma \geq 0} L(x, y, z, \sigma, \lambda), \forall \lambda_l \geq 0, \\ & 0 \geq \min_{\sigma \geq 0} G(x, y, z, \sigma, \mu), \forall \mu_l \in \Lambda \\ & x_l, y_l, z_l \in \{0, 1\}, \forall l \in \mathcal{L}. \end{aligned} \quad (10)$$

Note that the master problem has two inner optimization problems as its constraints, which need to be considered for all λ and μ . This implies that the master problem has a very large number of constraints. In [10], following relaxation has been proposed for the master problem at iteration m as

$$M(\sigma, \lambda, \mu) \begin{cases} \max \beta \\ \text{s.t.} & \beta \leq \tilde{L}(x^{(n)}, y^{(n)}, z^{(n)}, \sigma^{(n)}, \lambda^{(n)}), \forall n \in P^m \\ & 0 \geq \tilde{G}(x^{(n)}, y^{(n)}, z^{(n)}, \sigma^{(n)}, \mu^{(n)}), \forall n \in F^m. \\ & x_l, y_l, z_l \in \{0, 1\}, \forall l \in \mathcal{L}. \end{cases} \quad (11)$$

where the relaxed constraints are given respectively by

$$\begin{aligned} \tilde{L}(x^{(n)}, y^{(n)}, z^{(n)}, \sigma^{(n)}, \lambda^{(n)}) &= L(x^{(n)}, y^{(n)}, z^{(n)}, \sigma^{(n)}, \lambda^{(n)}) \\ &+ \nabla_x L(x^{(n)}, y^{(n)}, z^{(n)}, \sigma^{(n)}, \lambda^{(n)})(x - x^{(n)}) \\ &+ \nabla_y L(x^{(n)}, y^{(n)}, z^{(n)}, \sigma^{(n)}, \lambda^{(n)})(y - y^{(n)}) \\ &+ \nabla_z L(x^{(n)}, y^{(n)}, z^{(n)}, \sigma^{(n)}, \lambda^{(n)})(z - z^{(n)}) \end{aligned}$$

and

$$\begin{aligned} \tilde{G}(x^{(n)}, y^{(n)}, z^{(n)}, \sigma^{(n)}, \mu^{(n)}) &= G(x^{(n)}, y^{(n)}, z^{(n)}, \sigma^{(n)}, \mu^{(n)}) \\ &+ \nabla_x G(x^{(n)}, y^{(n)}, z^{(n)}, \sigma^{(n)}, \mu^{(n)})(x - x^{(n)}) \\ &+ \nabla_y G(x^{(n)}, y^{(n)}, z^{(n)}, \sigma^{(n)}, \mu^{(n)})(y - y^{(n)}) \\ &+ \nabla_z G(x^{(n)}, y^{(n)}, z^{(n)}, \sigma^{(n)}, \mu^{(n)})(z - z^{(n)}) \end{aligned}$$

P^m and F^m are the set of feasible and infeasible primal problems solved up to iteration m :

$$\begin{aligned} P^m &:= \{n \leq m : P(x^{(n)}, y^{(n)}, z^{(n)}) \text{ is feasible}\} \\ F^m &:= \{n \leq m : F(x^{(n)}, y^{(n)}, z^{(n)}) \text{ is infeasible}\} \end{aligned} \quad (12)$$

B. GBD algorithm

The GBD algorithm is operated in an iterative way as shown in Algorithm 1. In each iteration m , the optimal primal-dual pair $(\sigma^{(m)}, \lambda^{(m)})$ (for feasible primal problem) or $(\sigma^{(m)}, \mu^{(m)})$ (for infeasible primal problem) are solved with fixed integer variables $(x^{(m)}, y^{(m)}, z^{(m)})$, which are fed into (11) to solve the master problem. Since $M(\sigma^{(m)}, \lambda^{(m)}, \mu^{(m)})$ is a relaxation of master problem in (10), it provides an upper bound to (10) and can be used to generate the primal problem in the next iteration, and same procedure is repeated. The sequence of upper bounds in GBD is non-increasing and the set of lower bounds in GBD is nondecreasing, and the domain of the binary variables are finite. The two sequences are proven to converge and the algorithm will stop at the optimal solution $(x^*, y^*, z^*, \sigma^*)$ within a finite number of iterations [5], [10].

The primal problem can be solved using dual decomposition for practical implementation. Let us consider the feasible primal case, from (2) and (5), we have

$$\begin{aligned} L(\hat{x}, \hat{y}, \hat{z}, \sigma, \lambda) &= \sum_{l \in \mathcal{L}} U_l(\sigma_l) + \sum_{l \in \mathcal{L}} \lambda_l (1 - T_l(\hat{x}, \hat{y}, \hat{z}, \sigma)) \\ &= \sum_{l \in \mathcal{L}} U_l(\sigma_l) + \sum_{l \in \mathcal{L}} \lambda_l \left(1 - \frac{A_l}{C_l} - \sum_{l' \in I_l^s} \frac{x_{l'}^i A_{l'}}{C_{l'}} \right. \\ &\quad \left. - \sum_{l' \in I_l^t} \frac{y_{l'}^j A_{l'}}{C_{l'}} - \sum_{l' \in I_l^f} \frac{z_{l'}^k A_{l'}}{C_{l'}} \right) \\ &= \sum_{l \in \mathcal{L}} \left(U_l(\sigma_l) - \gamma_l \frac{A_l}{C_l} \right) + \sum_{l \in \mathcal{L}} \lambda_l \\ &= \sum_{l \in \mathcal{L}} L_l(\sigma_l) + \sum_{l \in \mathcal{L}} \lambda_l \end{aligned}$$

where

$$\gamma_l = \lambda_l + \sum_{l' \in I_l^s} \lambda_{l'} x_{l'}^i + \sum_{l' \in I_l^t} \lambda_{l'} y_{l'}^j + \sum_{l' \in I_l^f} \lambda_{l'} z_{l'}^k$$

is the aggregate multipliers of links conflicting with link l over radio and channel, and $L_l(\sigma_l) = U_l(\sigma_l) - \gamma_l \frac{A_l}{C_l}$ is the Lagrangian of link l .

Given γ_l , each link l can obtain σ_l by solving its Lagrangian function as follows

$$\sigma_l(\gamma_l) = \arg \max_{\sigma_l \geq 0} \left[U_l(\sigma_l) - \gamma_l \frac{A_l}{C_l} \right], \forall l \in \mathcal{L}. \quad (13)$$

The Lagrangian multipliers can be obtained from the dual problem as

$$\min_{\lambda \geq 0} \sum_{l \in \mathcal{L}} L_l(\sigma_l) + \sum_{l \in \mathcal{L}} \lambda_l \quad (14)$$

which can be solved using the following gradient method,

$$\lambda_l = [\lambda_l - \alpha(1 - T_l(\hat{x}, \hat{y}, \hat{z}, \sigma))]^+ \quad (15)$$

where α is a sufficiently small positive step size, and $[\cdot]^+$ denotes the projection onto the nonnegative orthant.

Algorithm 1: GBD Algorithm

input : Link-level demand $A_l, \forall l \in \mathcal{L}$.

output: Radio and channel assignment (x^*, y^*, z^*) and interference margin σ^* .

begin

Set $m = 1$ and choose $x^{(m)}, y^{(m)}, z^{(m)} \in \{0, 1\}$.
 $LB^0 \leftarrow -\infty, UB^0 \leftarrow \infty, P^0 \leftarrow \emptyset, F^0 \leftarrow \emptyset$.

while $LG^{m-1} < UB^{m-1}$ **do**

if the primal problem is feasible **then**

 Solve the primal problem $P(x^{(m)}, y^{(m)}, z^{(m)})$ to obtain optimal solution $\sigma^{(m)}$ and $\lambda^{(m)}$;

$P^m \leftarrow P^{m-1} \cup \{m\}, F^m \leftarrow F^{m-1}$;

$LB^m \leftarrow \max(LB^{m-1}, v(x^{(m)}, y^{(m)}, z^{(m)}))$;

if $LB^m = v(x^{(m)}, y^{(m)}, z^{(m)})$ **then**

$(x^*, y^*, z^*, \sigma^*) \leftarrow (x^{(m)}, y^{(m)}, z^{(m)}, \sigma^{(m)})$;

end

else if the primal problem is infeasible **then**

 Solve the feasibility-check problem

$F(x^{(m)}, y^{(m)}, z^{(m)})$ to obtain the optimal solution $\sigma^{(m)}$ and $\mu^{(m)}$;

$P^m \leftarrow P^m, F^m \leftarrow F^{m-1} \cup \{m\}$;

end

 Solve the master problem $M(\sigma^{(m)}, \lambda^{(m)}, \mu^{(m)})$

 to obtain the optimal solution $(x^{(m+1)}, y^{(m+1)}, z^{(m+1)})$ and $\beta^{(m)}$;

$UB^m \leftarrow \beta^{(m)}, m \leftarrow m + 1$;

end

return (x^*, y^*, z^*) and σ^* .

Similar approach can be used for the infeasible primal problem, the details are omitted here due to space limit. In this way, the primal problem can be solved distributively by each link by exchanging Lagrangian multipliers with neighboring links. The resulting interference margin and Lagrangian multipliers need to be reported to a central server or cluster head to solve the master problem. In this case, the information that needs to be transmitted is constant, and the communication cost is low.

C. Effective link rate under Gaussian noise channel model

To solve the MINLP problem (4) using the GBD algorithm, the problem should be convex with respect to the interference margin variables for fixed integer variables, which may not hold in general. However, for the AWGN channel, the effective link rate is known to be upper bounded by Shannon's capacity formula as $C_l = \log(1 + SINR_l)$. When the SINR is relatively higher, using the approximation $\log(1 + x) \approx \log(x)$, we can apply the geometric programming techniques [3] and let $\tilde{\sigma}_l = \log(\sigma_l)$. The link capacity can be expressed as

$$C_l = \log \left(\frac{P_s \bar{G}_{st}}{\sigma_0 + e^{\tilde{\sigma}_l} + \sum_{s' \neq s} P_{s'} \bar{G}_{s't}} \right) \quad (16)$$

which becomes a concave function of $\tilde{\sigma}_l$. Substituting (16) into (4), then the problem is convex with respect to $\tilde{\sigma}_l$ s since each constraint is a nonnegative weighted sum of a set of

convex functions $A_l/C_l\tau$, which preserves the convexity of these functions.

D. Scheduling

Given the radio and channel assignment results, it remains to decide when a link should be scheduled for packet transmission. We devise a TDMA schedule so that in each time slot only a set of conflict-free links are scheduled for transmission. Let n_l denote the number of slots required by a link l , which is given by $n_l = \lceil A_l/C_l\tau \rceil$, where τ is the slot duration. Let I_l denote the set of links conflicting with link l . For a time slot t , let $S(t)$ denote the set of links assigned in this time slot, and $F(t)$ denote the remaining links yet to be assigned. The scheduling algorithm works as in Algorithm 2.

Algorithm 2: Time Slot Scheduling Algorithm

input : Slot demand n_l and conflicting set $I_l, \forall l \in \mathcal{L}$.

output: Time slot assignment S .

```

begin
   $t \leftarrow 0$ ;
  while there exists a link  $l \in \mathcal{L}$  with  $n_l > 0$  do
     $S(t) \leftarrow \emptyset, F(t) \leftarrow \{l | n_l > 0, l \in \mathcal{L}\}$ .
    while  $F(t) \neq \emptyset$  and  $n_l > 0, \forall l \in F(t)$  do
      Select a link  $l \in F(t)$  and set
       $l^* \leftarrow \arg \max_{l \in F(t)} n_l$ ;
       $S(t) \leftarrow S(t) \cup \{l^*\}$ ;
       $F(t) \leftarrow F(t) \setminus (\{l^*\} \cup I_{l^*})$ ;
       $n_{l^*} \leftarrow n_{l^*} - 1$ ;
    end
     $t = t + 1$ ;
  end
  return  $S$ .
end

```

The above algorithm is essentially a maximal scheduling, where in each time slot, the set of links belonging to a maximal independent set are scheduled. Maximal scheduling yields simple distributed implementations [4], [21].

V. PERFORMANCE EVALUATION

In this section, we evaluate the performance of the proposed *Robust* radio and channel assignment scheme using real-world traces. For comparison purpose, we have implemented two traffic-agnostic algorithms as baselines.

- The *MinInt* algorithm is a modified channel assignment scheme based on the Gibbs sampler algorithm proposed in [11] that minimizes the network interference.
- The *Random* algorithm assigns the radios and channels for individual links randomly.

In the experiments, all the nodes have the same number of radios varying between 1 and 3, and the same number of channels varying from 1 to 4. Twenty set of link-level traffic demand vectors are randomly generated as inputs, and the final results show both the average value and standard deviation for all experiments. For the *Random* assignment algorithm, each set of experiments are repeated ten times with different radio and channel assignment results and their average is plotted.

The input of RSS for each link is the average value from the measurement.

A. Trace collection

A wireless mesh testbed with 11 nodes has been setup to run wireless experiments at University of Houston. Each node is an embedded Wireless Router Application Platform (WRAP) board with 233 MHz AMD Geode SC1100 CPU, 64Mb DRAM, with two Mini PCI Atheros 802.11a/b/g wireless cards and one Ethernet port. A snap shot of the real time connectivity map of the testbed is shown in Fig. 2(a).

We conduct multiple rounds of measurements to collect the received signal strength (RSS) profiles for the testbed. In each round, only one node is allowed to broadcast 100 UDP packets of 12 bytes payload at the lowest data rate (1Mbps), other nodes are working in monitor mode and can obtain the RSS from each received packet using the radiotap header in MADWIFI driver [1]. The experiments were repeated and lasted for 24 hours.

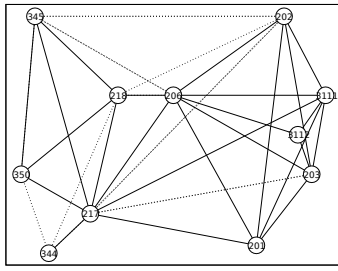
Fig. 2(b) gives a snap shot of the instantaneous RSS measurements of two links in our testbed. Using the collected data, we create the CDF of the RSS for each link in the testbed (Fig. 2(c)). The average RSS values are used as inputs for the radio and channel assignment algorithm, whereas the RSS profiles are used to generate test cases to evaluate the robustness of the resulting channel assignments.

From the RSS measurements, we can observe that the RSS values have significant variations on a short time scale even for the link with the strongest average signal strength. This motivate us to design robust channel algorithm to maximize link interference margins so that moderate variations in received signal strength can be tolerated without violating link-level traffic demands.

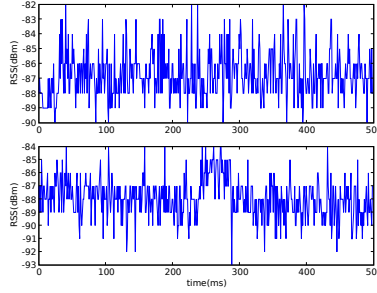
B. Trace-driven numerical results

1) *Interference margin*: We first evaluate the interference margin obtained from the three algorithms. To compute interference margins and link rate vector for the *MinInt* and *Random* algorithms, we take the radio and channel assignment results returned by these two algorithms as inputs to our algorithm and skip the radio and channel assignment step. Note that rate selection is not considered in the original *MinInt* algorithm [11] and *Random* algorithms. Therefore, the comparison in fact errs on the side of favoring these two algorithms.

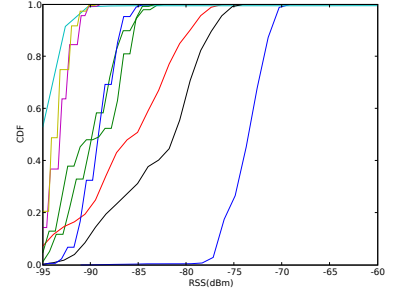
Fig. 3 shows the interference margin obtained by three algorithms with various setting of radios (1 to 3) and channels (1 to 4). The interference margin is computed as the minimum value among all links in the same setting on all experiments. We can see that *Robust* algorithm outperforms other two schemes in providing larger interference margin as expected. Among the three, the performance of *Random* algorithm is the worst because it is agnostic to both link-level demand as well as interference levels. *MinInt* algorithm performs better than *Random* algorithm since it tries to minimize the co-channel interference. As the number of radios and channels increases,



(a) Testbed topology

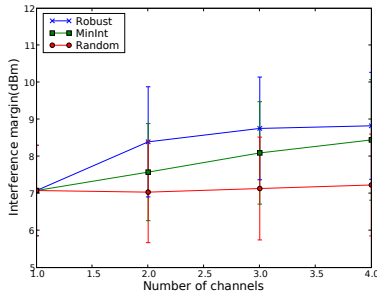


(b) Real time traces of received signal strength

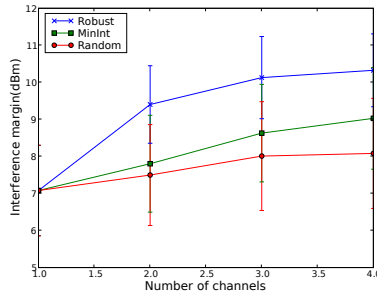


(c) CDF of received signal strength on a subset of links

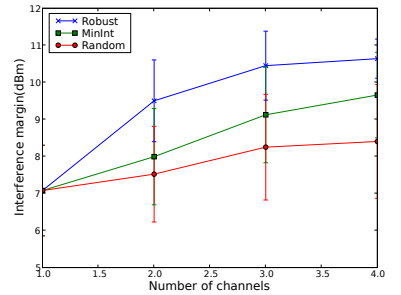
Fig. 2: Testbed topology and trace of received signal strength



(a) One radio



(b) Two radios



(c) Three radios

Fig. 3: Interference margin vs. the number of channels and radios

the interference margin attainable by all schemes increases. However, the increments tend to flatten out for more radios and channels.

2) *Robustness to channel variability*: Next, we evaluate the impact of channel variation on the performance of these three algorithms. As stated earlier, the channel assignment decision is made based on the average RSS values on all links. However, from the measurement study in the previous section, we observe significant short-term variability. One interesting question is thus, fixing the link-level demand, *does the channel assignment (based on average RSS) remain valid over time?* To this end, we introduce the *outage probability* metric. A large number of RSS samples are generated for each link using its RSS CDF profile. For each set of RSS values, we compute the SINR for each individual links and obtain their transmission rates, with which we can check the radio and contention constraint (3) for each link. An *outage* occurs if this constraint is violated, and the overall *outage probability* is the percentage of violated constraints. We repeat this procedure 1000 times and obtain the outage probability under the three channel assignment algorithms in Fig. 4.

From Fig. 4, we see that that *Robust* algorithm incurs less outage probability than other two algorithms under most cases. Although our algorithm does not explicitly optimize for the outage probability (which is dependent on RSS variation over time), a larger interference margin generally provides higher allowance to link variability. This is consistent with

our intuition. It can also be observed from these figures that the outage probabilities are significantly reduced when more radios and channels are employed.

3) *Convergence time*: Fig. 5 shows the convergence behavior of the proposed algorithm for the case of 3 radios, 4 channels. In Fig. 5, the upper bound returned by the master problem decreases monotonically and converges to the lower bound obtained from the primal problem. Optimality is obtained at around 75 iterations. We observe that faster convergence can be achieved with smaller number of radios and channels; and the results are omitted due to space limit.

C. Trace-driven simulation results

In this section, we compare the performance of the three radio and channel assignment algorithms using the Qualnet simulator [19]. We choose Qualnet because it has built-in multichannel support, and a node can change the channel it operates on from permitted set of channels at run time. Furthermore, Qualnet provides a PATHLOSS-MATRIX propagation model which incorporates a three-dimensional matrix indexed by source node, destination node, and time to calculate path loss between nodes. The 11-node testbed topology is used in the simulations. The TDMA MAC protocol in Qualnet is modified to allow transmission of multiple packets within a slot. The TDMA schedule is generated using the algorithm discussed in Section IV and imported to the simulation. Since 802.11a PHY only supports 8 transmission rates (6, 9, 12,

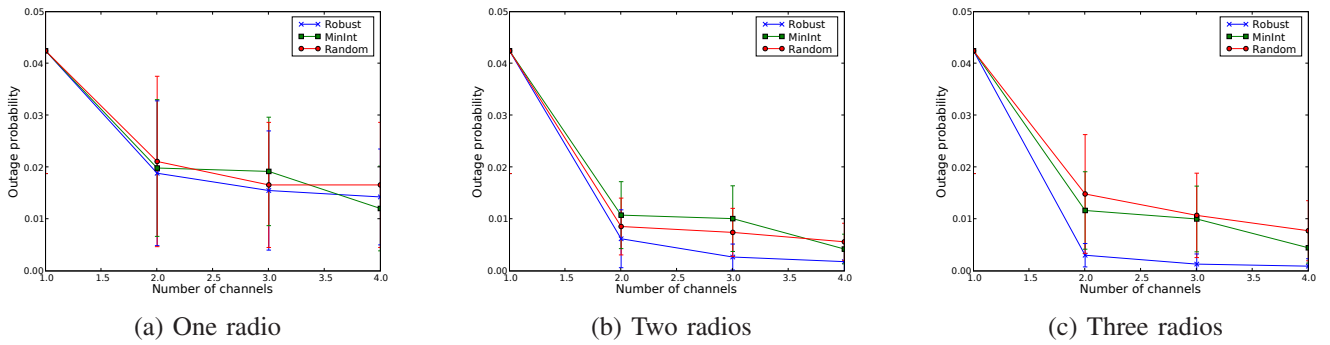


Fig. 4: Outage probability vs. the number of channels and radios

18, 24, 36, 48, 54Mbps), link rates obtained from the three algorithms are rounded to the next higher rate level supported by 802.11a and remain fixed throughout the simulation runs.

To study the effects of external interference, we generate four interference sources located in the four corners of the testbed, each source can inject AWGN signals at -30dBm. We consider three scenarios for the activities of these interference sources:

- *No interference* – None of these interference sources is activated during the simulation.
- *Random interference* – Only one of the randomly selected interference sources is activated in each time slot.
- *Persistent interference* – All interference sources are activated during the simulation.

Fig. 6 shows the packet loss probability obtained by three algorithms for the case that no interference source is activated. In this case, packet losses are mainly due to the channel variations. We see that *Robust* algorithm incurs less packet losses than other two algorithms under most cases. This is consistent with the numerical results in previous subsection where *Robust* algorithm can achieve higher interference margin than other two algorithms, which allows higher tolerance to channel variability.

Fig. 7 and 8 show the results for random and persistent interference cases respectively. As expected, due to the existence of external interference and channel variation, the packet loss probabilities are higher than the previous experiments. It can be seen from these figures that the *Robust* algorithm achieves better performance than the other two schemes. This demonstrates that the proposed algorithm is more robust to channel variations and external interference than other schemes.

VI. CONCLUSIONS

In this paper, we proposed a robust radio and channel assignment algorithm for MC-MR wireless networks that considers the realistic channel conditions, network resource constraints and link-level demands. To quantify the degree of robustness, we introduced the novel concept of “interference margin”. By optimizing the utility of interference margin subject to link-level demands, we demonstrated numerically and experimentally that robustness to channel variability and external interference sources can be achieved.

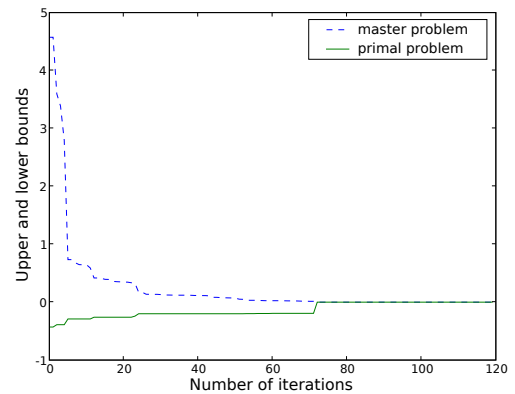


Fig. 5: Upper and lower bounds vs. Iteration(3 radios, 4 channels)

As part of on-going work, we are extending the proposed algorithm to transmission power control and other robust resource provision problems in multihop wireless networks.

REFERENCES

- [1] Madwifi, multiband atheros driver for wifi. <http://madwifi.org/>.
- [2] M. Alicherry, R. Bhatia, and L. E. Li. Joint channel assignment and routing for throughput optimization in multi-radio wireless mesh networks. In *MobiCom'05*, pages 58–72. ACM, 2005.
- [3] S. Boyd, S.-J. Kim, L. Vandenberghe, and A. Hassibi. A tutorial on geometric programming. *Optimization and Engineering.*, 8:67–127, 2007.
- [4] P. Chaporkar, K. Kar, X. Luo, and S. Sarkar. Throughput and fairness guarantees through maximal scheduling in wireless networks. *IEEE Transactions on Information Theory*, 54(2):572–594, 2008.
- [5] A. M. Geoffrion. Generalized benders decomposition. *Journal of Optimization Theory and Applications*, 10(4):237–260, 1972.
- [6] K. Jain, J. Padhye, V. N. Padmanabhan, and L. Qiu. Impact of interference on multi-hop wireless network performance. In *MobiCom'03*, pages 66–80. ACM, 2003.
- [7] A. Kashyap, S. Ganguly, and S. R. Das. A measurement-based approach to modeling link capacity in 802.11-based wireless networks. In *MobiCom'07*, pages 242–253, New York, NY, USA, 2007. ACM.
- [8] B. Kauffmann, F. Baccelli, A. Chaintreau, V. Mhatre, K. Papagiannaki, and C. Diot. Measurement-based self organization of interfering 802.11 wireless access networks. In *IEEE INFOCOM'07*, pages 1451–1459, 2007.
- [9] M. Kodialam and T. Nandagopal. Characterizing the capacity region in multi-radio multi-channel wireless mesh networks. In *MobiCom'05*, pages 73–87. ACM, 2005.
- [10] D. Li and X. Sun. *Nonlinear Integer Programming*. Springer, 2006.

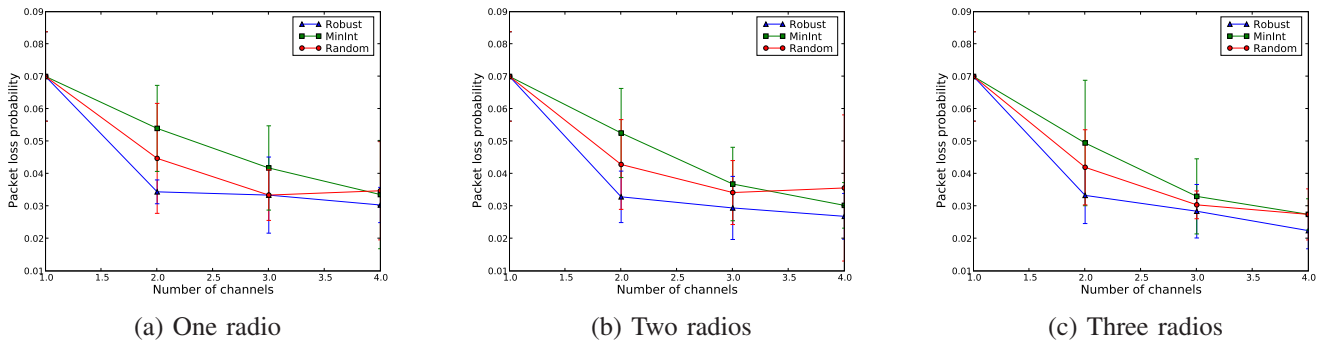


Fig. 6: Packet loss probability vs. the number of channels and radios(no interference case)

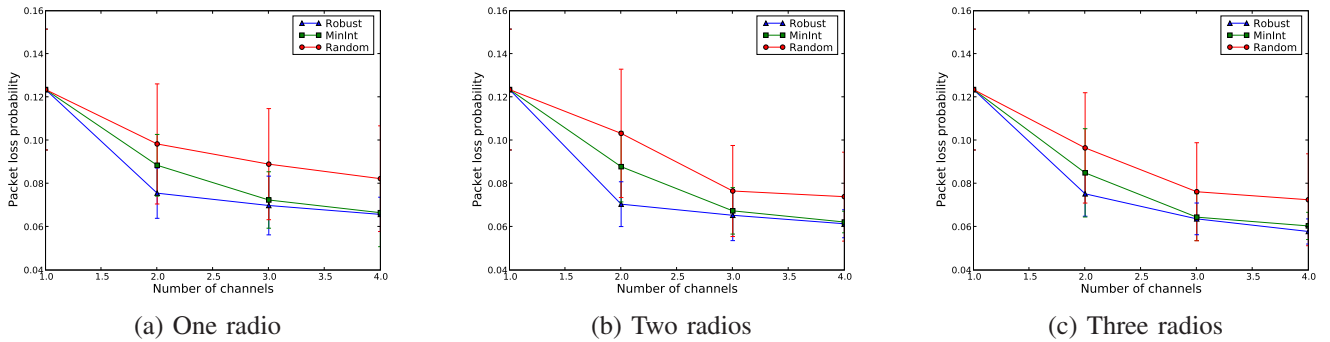


Fig. 7: Packet loss probability vs. the number of channels and radios(random interference case)

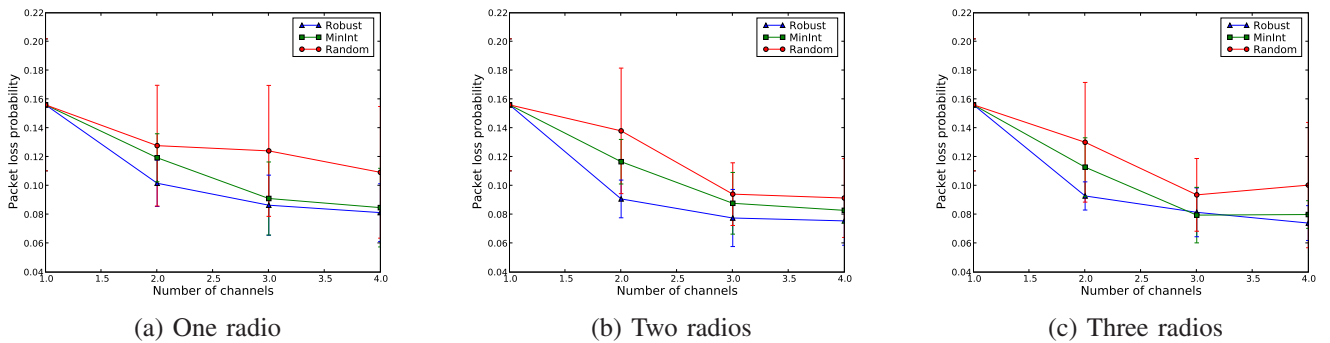


Fig. 8: Packet loss probability vs. the number of channels and radios(persistent interference case)

- [11] V. P. Mhatre, K. Papagiannaki, and F. Baccelli. Interference mitigation through power control in high density 802.11 WLANs. In *IEEE INFOCOM'07*, pages 535–543, 2007.
- [12] J. Padhye, S. Agarwal, V. N. Padmanabhan, L. Qiu, A. Rao, and B. Zill. Estimation of link interference in static multi-hop wireless networks. In *IMC'05*, pages 28–28. USENIX Association, 2005.
- [13] L. Qiu, Y. Zhang, F. Wang, M. K. Han, and R. Mahajan. A general model of wireless interference. In *MobiCom'07*, pages 171–182. ACM, 2007.
- [14] A. Rad and V. Wong. Joint channel allocation, interface assignment and mac design for multi-channel wireless mesh networks. *IEEE INFOCOM'07*, pages 1469–1477, May 2007.
- [15] B. Radunovic and J.-Y. Le Boudec. Rate performance objectives of multihop wireless networks. *IEEE INFOCOM'04*, 3:1916–1927 vol.3, March 2004.
- [16] A. Raniwala, K. Gopalan, and T. Chiueh. Centralized channel assignment and routing algorithms for multi-channel wireless mesh networks. *SIGMOBILE Mob. Comput. Commun. Rev.*, 8(2):50–65, 2004.
- [17] C. Reis, R. Mahajan, M. Rodrig, D. Wetherall, and J. Zahorjan. Measurement-based models of delivery and interference in static wireless networks. *SIGCOMM Comput. Commun. Rev.*, 36(4):51–62, 2006.
- [18] E. Rozner, Y. Mehta, A. Akella, and L. Qiu. Traffic-aware channel assignment in enterprise wireless LANs. In *Proc. of ICNP*, 2007.
- [19] I. Scalable Network Technologies. *QualNet 4.0 Programmer's Guide*. Scalable Network Technologies, Inc., 2007.
- [20] A. P. Subramanian, H. Gupta, and S. R. Das. Minimum interference channel assignment in multi-radio wireless mesh networks. In *IEEE SECON'07*, pages 481–490, 2007.
- [21] X. Wu, R. Srikant, and J. R. Perkins. Scheduling efficiency of distributed greedy scheduling algorithms in wireless networks. *IEEE Trans. on Mobile Computing*, 6(6):595–605, June 2007.
- [22] Y. Xi and E. M. Yeh. Distributed algorithms for spectrum allocation, power control, routing, and congestion control in wireless networks. In *MobiHoc'07*, pages 180–189. ACM, 2007.
- [23] G. Zussman, A. Brzezinski, and E. Modiano. Multihop local pooling for distributed throughput maximization in wireless networks. In *IEEE INFOCOM'08*, 2008.